Novel Styrylpyridines as Probes for SPECT Imaging of Amyloid Plaques

Wenchao Qu,[†] Mei-Ping Kung,[†] Catherine Hou,[†] Tyler E. Benedum,[‡] and Hank F. Kung[*,†,§]

Departments of Radiology and Pharmacology, University of Pennsylvania, Philadelphia, Pennsylvania 19104, and Avid Radiopharmaceuticals, Inc., Philadelphia, Pennsylvania 19104

We report a series of radioiodinated styrylpyridines as single photon emission computed tomography probes for imaging Aβ plaques in the brain of patients with Alzheimer's disease (AD). In vitro binding showed that all of the styrylpyridines displayed very good binding affinities in postmortem AD brain homogenates (K_i = 3.6 to 15.5 nM). No-carrier-added samples of **13a**, **13b**, **16a**, **16b**, and **16e** (radioiodinated with ^{125}I) were successfully prepared. The in vivo biodistribution in normal mice, at 2 min after injection, showed excellent initial brain penetrations (4.03, 6.22, 5.43, and 8.04% dose/g for [^{125}I]**13a**, **13b**, **16a**, and **16b**, respectively). Furthermore, in vitro autoradiography of AD brain sections showed that the high binding signal was specifically due to the presence of Aβ plaques. Taken together, these results strongly suggest that these styrylpyridines are useful for imaging Aβ plaques in the living human brain.

Introduction

Alzheimer's disease (AD[a]) is an insidious neurodegenerative disease of the brain. It is an increasingly significant medical problem with a high prevalence in millions of elderly people. Major neuropathological observations of postmortem AD brains reveal the presence of senile plaques (containing β-amyloid (Aβ) aggregates) and neurofibrillary tangles (highly phosphorylated tau proteins).[1−6] An excessive burden of Aβ produced by various normal or abnormal mechanisms may represent the starting point of neurodegenerative events. The formation of soluble and diffusible Aβ[7] and Aβ aggregates associated with the neuritic plaques in the brain produce various toxic effects in neuronal cells.[6,8−11] Currently, it is difficult for clinicians to differentiate between the cognitive decline associated with normal aging and the cognitive decline associated with AD. Aside from postmortem pathological staining of the brain tissue, there is no simple and definitive diagnostic method to detect Aβ plaques in the brain. Thus, development of positron emission tomography (PET) or single photon emission computed tomography (SPECT) imaging agents, which could measure Aβ plaques in the living brain may assist with early diagnosis of AD.

In the past few years, successful PET imaging studies with [11C]PIB, **1**, in AD patients have been reported.[12−21] Recently, ligand [11C]**1** (Figure 1) has also been used in a limited number of patients with mild cognitive impairment (MCI).[15,22,23] Using **1**/PET, it is possible to study the relationship between Aβ plaque burden and neurological symptoms of AD. The results seem to suggest that while some MCI cases convert to AD, those with lower **1** uptake in the cortex appear to be less likely to convert to AD.[19,21,24−26] In addition to the promising data obtained with [11C]**1**, in human PET studies using [11C]SB-13,[27] **2**, and [18F]FDDNP,[28−30] **3**, significant differences in the labeling of AD and age-matched control patients have been observed.

Currently, there are extensive infrastructures set up for SPECT imaging studies in major medical centers and community hospitals. If appropriate, SPECT imaging agents targeting Aβ plaques could be developed; they would be useful for widespread diagnosis and monitoring of AD patients. The development of this series of novel SPECT imaging agents would therefore benefit a large number of patients. We, and others, have reported several radioiodinated ligands based on benzothiazole backbone structures.[31−33] However, most of these ligands had slow in vivo washouts resulting in high background-to-noise ratios, thus preventing their further development as potential in vivo imaging agents. Subsequently, our search for potential SPECT imaging agents extended from thioflavins to the stilbene series[34] and to the highly rigid tricyclic fluorene series,[35] with relatively limited success.

The development of [123I]IMPY, **4**, a unique thioflavin derivative with a [1,2,*a*]imidazopyridine ring, showed the feasibility of developing SPECT imaging agents for targeting Aβ plaques.[36−38] However, ligand [123I]**4** had certain undesirable characteristics that prompted us to pursue the development of a second generation of [123I] SPECT imaging agents. In preliminary clinical data, AD patients showed a higher uptake of [123I]-**4** in comparison with control subjects.[39] However, the target-to-background ratio for plaque labeling was not as high as that of **1**. In AD patients, ligand **1** showed a *S/N* ratio of about 2.5,[15,25] while **4** displayed a ratio of 1.4 to 1.6 (30−50 min after an iv injection).[40] This lower specific signal may be due to the relatively fast brain and plasma clearance observed in AD as well as in normal subjects. It could also be the result of the in vivo metabolism or the in vivo instability of [123I]**4** (unpublished data). While the clinical study of [123I]**4** in normal and AD patients is ongoing, we are seeking to improve the signal-to-noise ratio by searching for a second generation of [123I] SPECT agents with better kinetics and an increased target-to-background ratio.

We have recently developed two new PET tracers based on stilbene and styrylpyridine core structures containing fluoro-

* To whom correspondence should be addressed. Hank F. Kung, Ph.D., Department of Radiology, University of Pennsylvania, 3700 Market Street, Room 305, Philadelphia, Pennsylvania 19104. Tel.: (215) 662-3096. Fax: (215) 349-5035. E-mail: kunghf@sunmac.spect.upenn.edu.
† Department of Radiology, University of Pennsylvania.
‡ Avid Radiopharmaceuticals, Inc.
§ Department of Pharmacology, University of Pennsylvania.
[a] Abbreviations: SPECT, single photon emission computed tomography; PET, positron emission tomography; AD, Alzheimer's disease; MCI, mild cognitive impairment; Aβ, β-amyloid; PIB, 2-(4′-(methylaminophenyl)-6-hydroxybenzothiazole; SB-13, 4-N-methylamino-4′-hydroxystilbene; FDD-NP, 2-(1-{6-[(2-fluoroethyl)methyl-amino]-2-naphthyl}ethylidend)-malononitrile; IMPY, 6-iodo-2-(4′-dimethylamino-)phenyl-imidazo[1,2-a]pyridine; PEGN3-SB, {4-[2-[4-{2-[2-(2-Fluoro-ethoxy)-ethoxy]-ethoxy}-phenyl)-vinyl]-phenyl}-methylamine; Styrylpyridine, (E)-2-(2-(2-(2-fluoroethoxy)ethoxy)ethoxy)-5-(4-dimethylaminostyryl)-pyridine; FPEG, fluoro-polyethyleneglycol.
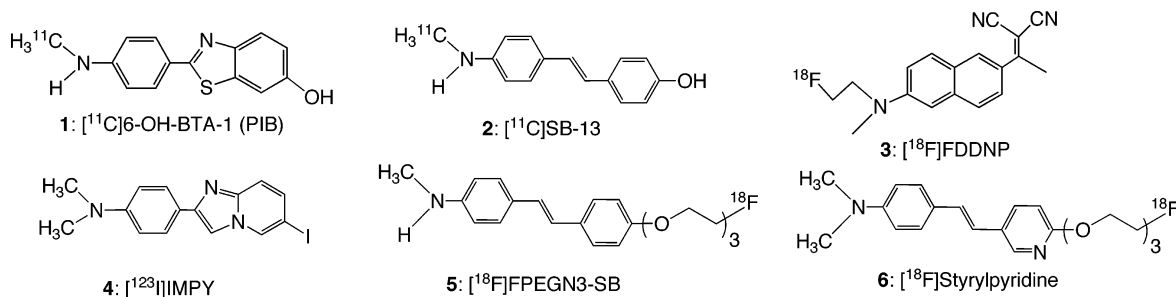
Figure 1. Chemical structures of various PET and SPECT ligands targeting Aβ plaque. 6-OH-BTA-1 (PIB), 2-(4′-(methylaminophenyl)-6-hydroxybenzothiazole; SB-13, 4-*N*-methylamino-4′-hydroxystilbene; FDDNP, 2-(1-[6-[(2-fluoroethyl)methyl-amino]-2-naphthyl]ethylidend)malononitrile; IMPY, 6-iodo-2-(4′-dimethylamino-)phenyl-imidazo[1,2-*a*]pyridine; PEGN3-SB, (*E*)-4-(4-(2-(2-(2-fluoroethoxy)ethoxy)ethoxy)styryl)-*N*-methylbenzenamine; styrylpyridine, (*E*)-4-(2-(6-(2-(2-(2-fluoroethoxy)ethoxy)ethoxy)pyridin-3-yl)vinyl)-*N*,*N*-dimethylbenzenamine.

Scheme 1[a]
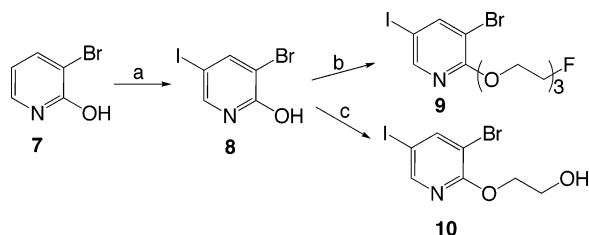
[a] Reagents and conditions: (a) NIS, CH₃CN, reflux, 1 h; (b) F(CH₂CH₂O)₃H, Ph₃P, DIAD, THF, −5 °C to rt, 2 h; (c) (1) HOCH₂CH₂OTBDMS, Ph₃P, DIAD, THF, −5 °C to rt, 2 h; (2) 1% HCl in 95% EtOH, rt, 1 h.

Table 1. Potencies (K_i) of Compounds on Competition of [^{125}I]**4** Binding to Amyloid Plaques in AD Brain Homogenates[a]

cmpd	K_i (nM ± SEM)
11a	6.8 ± 1.4
11b	4.5 ± 0.9
11e	14.2 ± 3.8
13a	7.5 ± 0.8
13b	9.0 ± 1.0
13e	21 ± 8.0
14a	3.6 ± 0.8
14b	5.0 ± 1.6
14e	6.8 ± 0.8
16a	7.5 ± 1.5
16b	8.5 ± 2.5
16e	15.5 ± 0.5

[a] Each value was determined three times with duplicate for each measurement.

polyethyleneglycol (FPEG) substituents[41−43] (**5** and **6**) showing highly desirable Aβ-targeting properties for PET imaging. The in vivo biodistribution studies showed excellent brain penetration after iv injection in normal mice. We were able to modulate the lipophilicity and preserve the ability to penetrate the blood−brain barrier by using end-capped FPEG groups or simply an ethylene glycol derivative.[41,42] On the basis of these new findings, we hypothesized that if we created iodinated compounds with a pyridine ring instead of the phenyl ring of the stilbene, they would have good binding affinities, while the pyridine ring modulates the lipophilicity or improves brain penetration.[44] Initially, we tested the strategy by comparing iodine derivatives of stilbene and styrylpyridine derivatives. Combining both pegylation and a pyridine ring on stilbenes resulted in a highly successful method for designing suitable ^{123}I probes to target Aβ plaques in the brain. We report herein the synthesis and the initial biological characterizations of this new series of iodinated styrylpyridine derivatives targeting Aβ plaques in the brain.

Results and Discussion

Chemistry. The syntheses of styrylpyridine derivatives were readily accomplished by the reactions shown in Schemes 1 and 2. Iodination of 2-hydroxy-3-bromopyridine **7** with *N*-iodosuccinimide (NIS) in acetonitrile (MeCN) under a refluxing condition afforded **8** in 85% yield.[45] Mitsunobu reaction of **8** with monofluorated triethylene glycol provided O-alkylated **9** in 75% yield.[46] The ethylene glycol tethered intermediate **10** was prepared by a similar Mitsunobu reaction and followed by an acidic desilylation reaction.[47] The combined yield of the two steps was 68%.

The bromo-substituted styrylpyridine derivatives (**11a−d**, **14a,b**, and **14d**) were assembled by a palladium-catalyzed Heck coupling reaction of iodide **9** and **10** with different 4-substituted styrenes.[48,49] The phenolic intermediates, **11e** and **14e**, were obtained by deacetylation of **11d** and **14d** under a basic condition. We have also prepared the corresponding tributyltin

starting material for a radioiodination reaction. The desired organostannane compounds (**12a−c**, **12e**, **15a,b**, and **15e**) were prepared by using Pd(PPh₃)₄-catalyzed *trans*-stannylation from their bromide precursors.[50] The subsequent iododestannylation reaction afforded iodinated targets (**13a**, **13c**, **13e**, **16a,b**, and **16e**). However, we were surprised that we were not able to make **13b** directly by an iododestannylation reaction from **12b**.[51] The acidic deprotection of the Boc group on **6c** failed to give the desired product. Alternatively, the same reaction was carried out in the presence of trimethylsilyl triflate and 2,6-lutidine,[52] which resulted in a clean cleavage of the *N*-Boc group and led to the target molecule, **13b**, with an excellent yield (88%).

Radiolabeling. To make the desired ^{125}I-labeled **13a**, **13b**, **16a**, **16b**, and **16e**, the corresponding tributyltin starting materials, **12a**, **12b**, **15a**, **15b**, and **15e**, were prepared as the precursors for labeling (Scheme 2). Standard iododestannylaltion reactions, using sodium [^{125}I]iodide, hydrogen peroxide, and hydrochloric acid, were successfully applied to all five ligands with 25−50% overall yields (Scheme 3). The chemical identities of the ^{125}I-labeled ligands were confirmed by using authentic standards to show identical retention times on HPLC. The radiochemical purities of all of the purified ligands were greater than 95% and all had a high specific activity (no carrier added, approx. 2000 Ci/mmol). Due to the pyridine ring on the backbone structure for all the ligands, we observed lower labeling yields (50−70% after the EtOAc extraction) as well as lower initial radiochemical purities (60−70% before the HPLC purification). These values were lower as compared to the preparation of the corresponding stilbene series of ^{125}I-labeled ligands (unpublished data). Currently, we are trying to optimize the labeling conditions to increase the overall yield. It is likely that minor adjustments of the labeling procedure will result in improved radiochemical yields.

Scheme 2[a]

11: R_2=-(CH$_2$CH$_2$O)$_2$CH$_2$CH$_2$F, R_3=-Br
12: R_2=-(CH$_2$CH$_2$O)$_2$CH$_2$CH$_2$F, R_3=-SnBu$_3$
13: R_2=-(CH$_2$CH$_2$O)$_2$CH$_2$CH$_2$F, R_3=-I
14: R_2=-CH$_2$CH$_2$OH, R_3=-Br
15: R_2=-CH$_2$CH$_2$OH, R_3=-SnBu$_3$
16: R_2=-CH$_2$CH$_2$OH, R_3=-I

a: R_1=-N(CH$_3$)$_2$
b: R_1=-NH(CH$_3$)
c: R_1=-N(Boc)(CH$_3$)
d: R_1=-OCOCH$_3$
e: R_1=-OH
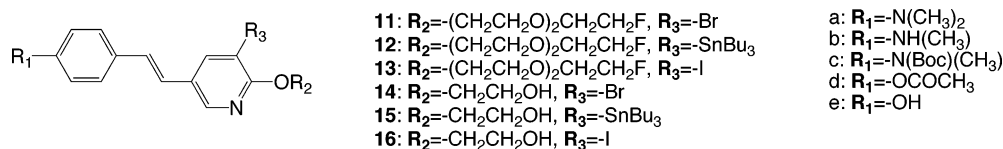
[a] Reagents and conditions: (a) 4-substituted styrenes, K$_2$CO$_3$, Bu$_4$NBr, Pd(OAc)$_2$, DMF, 55−65 °C; (b) (Bu$_3$Sn)$_2$, Pd(PPh$_3$)$_4$, toluene, 110 °C; (c) K$_2$CO$_3$, EtOH/ THF, rt, 2 h; (d) I$_2$, THF, 0 °C to rt; (e) TMSOTf, 2,6-lutidine, DCM, −78 °C to rt.

Scheme 3[a]

12a
12b
15a
15b
15e

[^{125}I]13a: R_1=-N(CH$_3$)$_2$, R_2=-(CH$_2$CH$_2$O)$_2$CH$_2$CH$_2$F
[^{125}I]13b: R_1=-NH(CH$_3$), R_2=-(CH$_2$CH$_2$O)$_2$CH$_2$CH$_2$F
[^{125}I]16c: R_1=-N(CH$_3$)$_2$, R_2=-CH$_2$CH$_2$OH
[^{125}I]16d: R_1=-NH(CH$_3$), R_2=-CH$_2$CH$_2$OH
[^{125}I]16e: R_1=-OH, R_2=-CH$_2$CH$_2$OH
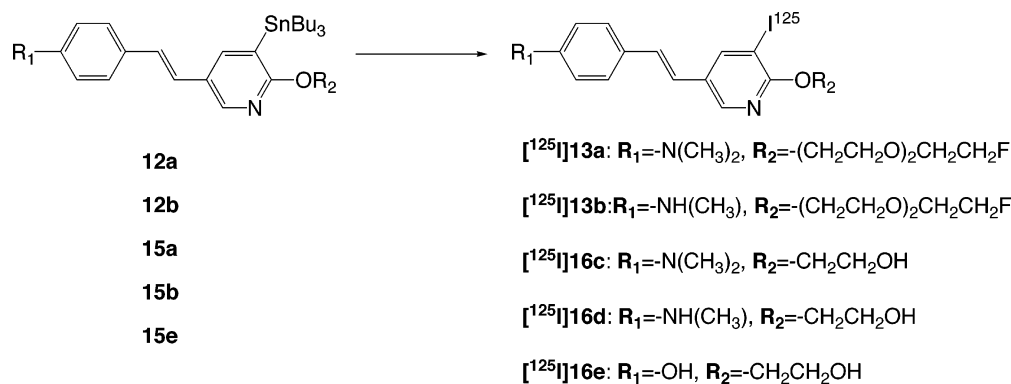
[a] Reagents and conditions: H$_2$O$_2$, NaI^{125}, HCl, EtOH.

Biological Evaluation. An in vitro binding assay serves as the first screening step for potential ligands targeting β-amyloid plaques. Successful assays have been developed with several PET and SPECT imaging agents with different core structures, including **2** and **4**, as well as several fluoropegylated stilbenes currently under clinical evaluation. The binding affinities (K_i, nM) of the iodinated styrylpyridine derivatives were first evaluated by a competitive binding assay with [^{125}I]**4** for Aβ plaques using homogenates prepared from postmortem AD brain tissues. All the iodinated styrylpyridine derivatives examined showed excellent-to-good binding affinities in comparison with [^{125}I]**4** binding. The addition of a fluoropegylated chain to the one end of the phenyl group did not affect the binding affinity to amyloid plaques. Compound **13a** showed a K_i value of 7.5 ± 0.8 nM (Table 1), which is comparable to a previously reported pyridine probe (K_i = 4.8 ± 0.6 nM[44]) containing a simple hydroxy substitution instead of an attached fluoropegylated chain. Similarly, the hydroxyl pegylated derivative, that is, **16a**, competed effectively with [^{125}I]**4** binding with a K_i value of 7.5 ± 1.5 nM. There is no significant difference in the binding affinities between *N,N*-dimethylamino derivatives, **13a**, **16a**, and *N*-monomethylamino derivatives, **13b**, **16b** (K_i = 9.0 ± 1.0 and 8.5 ± 2.5 nM, respectively). After replacing the substituted amino group with a hydroxy group attached to the 4-position of one end of the phenyl ring, the binding affinities showed a slight reduction (K_i = 21 ± 8.0 and 15.1 ± 0.5 nM for **13e** and **16e**, respectively). It was also evident that all of the brominated derivatives and the corresponding iodinated ligands displayed similar binding affinities (K_i values demonstrated in Table 1 between series **11**, **13**, **14**, and **16**).

On the basis of the encouraging binding data observed for **13a**, **13b**, **16a**, **16b**, and **16e**, we chose to carry out further biological evaluations using the ^{125}I-labeled styrylpyridines. All of the radioiodinated probes measured under the experimental conditions showed optimum partition coefficients (log P = 2.2−2.6), a desirable property for imaging agents. One exception is the hydroxy derivative, [^{125}I]**16e**, which displayed a lower partition coefficient (Log P = 1.98), leading to a low brain uptake (see the results of the animal study shown below). When evaluated for whole animal biodistribution after an iv injection in normal mice, [^{125}I]**13a**, **13b**, **16a**, and **16b** displayed good penetration of the intact blood−brain barrier with excellent initial brain uptakes (4.03, 6.22, 5.43, and 8.04% dose/g for [^{125}I]**13a**, **13b**, **16a**, **16b**, respectively at 2 min after a tracer injection). Compounds containing the hydroxy- or fluoro-peg group showed much higher brain penetrations as compared with the previously reported nonpegylated iodinated ligands.[44,53] These series of iodinated styrrylpyridines displayed superior brain penetration. The high brain uptakes of these iodinated ligands were subsequently followed by rapid washouts with less than 0.5% dose/g remaining in the brain at 2 h after the injection (Table 2). The brain washouts for the *N,N*-dimethylamino ligands, that is, [^{125}I]**13a** and [^{125}I]**16a**, were slower in comparison to the *N*-methylamino ligands, that is, [^{125}I]**13b** and [^{125}I]**16b** (Table 2). One way to select a ligand with appropriate in vivo kinetics is to use brain$_{2min}$/brain$_{30min}$ as the index to compare

Table 2. Biodistribution in Mice after IV Injections of [^{125}I]-Labeled Tracers[a]

[^{125}I]**13a** (log P = 2.59)			
organ	2 min	30 min	1 h	2 h
blood	2.70 ± 0.58	2.05 ± 0.18	1.65 ± 0.45	1.45 ± 0.41
heart	12.76 ± 1.24	1.63 ± 0.03	0.97 ± 0.16	0.73 ± 0.17
muscle	0.90 ± 0.20	1.00 ± 0.08	0.59 ± 0.13	0.53 ± 0.08
lung	10.1 ± 2.15	2.50 ± 0.14	1.62 ± 0.46	1.33 ± 0.39
kidney	16.6 ± 1.96	3.32 ± 0.11	2.30 ± 0.54	1.71 ± 0.24
spleen	4.47 ± 1.28	1.42 ± 0.05	0.99 ± 0.47	0.79 ± 0.27
liver	22.2 ± 4.34	9.54 ± 1.30	5.34 ± 2.22	5.62 ± 1.31
skin	0.54 ± 0.05	1.47 ± 0.26	1.59 ± 0.68	1.23 ± 0.41
brain	4.03 ± 0.43	1.93 ± 0.18	0.68 ± 0.17	0.26 ± 0.04
thyroid	3.89 ± 0.67	16.2 ± 11.75	24.2 ± 8.26	60.8 ± 6.09

[^{125}I]**13b** (log P = 2.54)			
organ	2 min	30 min[+]	1 h	2 h
blood	4.37 ± 1.07	3.83 ± 1.11	2.88 ± 0.28	2.21 ± 0.73
heart	9.85 ± 1.78	2.54 ± 0.37	1.75 ± 0.26	1.22 ± 0.28
muscle	1.04 ± 0.25	1.11 ± 0.34	0.85 ± 0.06	0.44 ± 0.19
lung	6.85 ± 0.27	3.01 ± 0.96	2.37 ± 0.29	1.85 ± 0.74
kidney	9.03 ± 6.81	3.40 ± 0.76	2.81 ± 0.70	1.86 ± 0.36
spleen	4.41 ± 1.05	2.49 ± 0.75	1.75 ± 0.33	1.27 ± 0.24
liver	26.2 ± 4.47	11.5 ± 2.10	7.70 ± 1.22	6.25 ± 1.79
skin	1.48 ± 0.27	2.95 ± 0.81	2.46 ± 0.16	1.32 ± 0.41
Brain	6.22 ± 1.01	1.23 ± 0.13	0.62 ± 0.17	0.26 ± 0.01
Thyroid	5.74 ± 0.42	24.1 ± 27.4	38.1 ± 6.37	215 ± 74.6

[^{125}I]**16a** (log P = 2.64			
organ	2 min	30 min	1 h[+]	2 h
blood	2.71 ± 0.07	2.24 ± 0.38	2.18 ± 0.66	1.01 ± 0.02
heart	10.2 ± 0.45	1.93 ± 0.27	1.12 ± 0.02	0.62 ± 0.12
muscle	0.71 ± 0.46	1.05 ± 0.20	0.55 ± 0.03	0.22 ± 0.04
lung	9.41 ± 0.56	3.02 ± 0.38	1.98 ± 0.21	1.00 ± 0.15
kidney	14.3 ± 1.98	4.19 ± 0.45	2.49 ± 0.33	1.48 ± 0.20
spleen	4.40 ± 1.89	1.94 ± 0.19	1.32 ± 0.10	0.80 ± 0.11
liver	19.1 ± 2.68	12.4 ± 1.29	6.22 ± 0.96	4.87 ± 0.46
skin	0.46 ± 0.13	1.18 ± 0.26	1.16 ± 0.00	0.40 ± 0.05
brain	5.43 ± 0.85	3.56 ± 0.32	1.32 ± 0.00	0.46 ± 0.05
thyroid	4.15 ± 0.43	11.2 ± 7.88	59.1 ± 6.26	24.8 ± 0.62

[^{125}I]**16b** (log P = 2.20)			
organ	2 min	30 min	1 h	2 h
blood	4.14 ± 0.41	3.08 ± 0.35	1.81 ± 0.56	1.96 ± 0.14
heart	7.16 ± 1.16	1.50 ± 0.18	0.88 ± 0.30	0.76 ± 0.03
muscle	1.15 ± 0.38	0.91 ± 0.06	0.42 ± 0.08	0.38 ± 0.02
lung	7.43 ± 1.21	2.67 ± 0.46	1.76 ± 0.32	1.58 ± 0.10
kidney	11.5 ± 1.48	3.73 ± 0.75	2.16 ± 0.08	1.53 ± 0.20
spleen	4.08 ± 0.68	1.34 ± 0.29	0.87 ± 0.37	1.08 ± 0.15
liver	20.8 ± 2.38	12.6 ± 3.03	5.62 ± 0.68	3.41 ± 0.20
skin	0.95 ± 0.09	1.86 ± 0.50	1.29 ± 0.51	1.43 ± 0.10
brain	8.04 ± 0.82	0.88 ± 0.30	0.26 ± 0.03	0.15 ± 0.02
thyroid	6.31 ± 1.59	17.2 ± 14.2	36.7 ± 37.2	99.9 ± 69.5

[^{125}I]**16e** (log P = 1.98)			
organ	2 min	30 min	1 h	2 h
blood	10.1 ± 1.12	3.92 ± 0.07	1.29 ± 0.05	1.56 ± 0.04
heart	6.66 ± 0.31	1.35 ± 0.16	0.65 ± 0.21	0.51 ± 0.09
muscle	1.01 ± 0.34	0.59 ± 0.05	0.21 ± 0.02	0.12 ± 0.01
lung	14.2 ± 0.92	3.10 ± 0.05	1.34 ± 0.11	1.02 ± 0.01
kidney	20.4 ± 2.20	10.0 ± 2.12	2.94 ± 0.17	2.50 ± 1.32
spleen	4.20 ± 0.31	1.28 ± 0.44	0.50 ± 0.03	0.50 ± 0.06
liver	18.3 ± 1.29	5.15 ± 0.61	2.38 ± 0.58	2.63 ± 1.30
skin	0.64 ± 0.20	1.36 ± 0.07	0.62 ± 0.01	0.37 ± 0.08
brain	0.99 ± 0.24	0.26 ± 0.03	0.09 ± 0.01	0.06 ± 0.01
thyroid	4.38 ± 0.46	3.99 ± 3.56	13.0 ± 8.11	16.0 ± 11.5

[a] %dose/g, avg of three mice $\pm$ SD.

Figure 2. In vitro autoradiography of macroarray brain sections constructed from six postmortem AD cases plus one control (marked by an arrowhead). Section labeling was carried out with four ^{125}I-labeled styrylpyridine ligands. Immunohistochemistry with 4G8 confirmed the presence and location of plaques in the sections (dots in the tissue section of the AD brain, but not in the control brain). Ligand [^{125}I]**4**, a well characterized SPECT ligand[37] targeting Aβ plaques, was included for comparison. Clearly, the Aβ plaques were successfully targeted by ^{125}I styrylpyridine derivatives **13a**, **13b**, **16a**, and **16b** with low background labeling.

the washout rate.[54,55] The four radiodinated styrylpyridine probes showed brain$_{2min}$/brain$_{30min}$ ratios of 2.09, 5.05, 1.52, and 9.13 for [^{125}I]**13a**, [^{125}I]**13b**, [^{125}I]**16a**, and [^{125}I]**16b**, respectively. According to this, the *N*-methylamino- derivatives, [^{125}I]-**13b** and [^{125}I]**16b**, which showed a high washout index, may

have better signal-to-noise ratios and therefore may be better for Aβ plaque detection. The low brain uptake observed for [^{125}I]**16e** may be due to either the presence of the additional hydroxy group on the molecule or to a lower partition coefficient.

Consistently, blood levels for all four radioiodinated ligands dropped gradually with time. A good initial brain uptake combined with a rapid washout (high brain$_{2min}$/brain$_{30min}$ ratio) in a normal mouse brain (presumably, there are no Aβ plaques in the normal mouse brain for extra binding by these Aβ plaque-targeting probes) is a highly desirable property. The radioiodinated styrylpyridine probes reported here, especially [^{125}I]**13b** and [^{125}I]**16b**, met this criteria and may be favorably considered as potential SPECT imaging agents for targeting Aβ plaques in vivo.

We also carefully constructed a group of human macro-array sections consisting of six confirmed AD cases and one control subject. After sectioning this macro-array, adjacent sections would reflect a comparable pathophysiology. In vitro film autoradiography was carried out using these ^{125}I-labeled styrylpyridine probes. Among the four styrylpyridine probes, [^{125}I]**13a** and **16a** exhibited the most distinctive plaque labeling with a minimal background (Figure 2). The labeling pattern was consistent with that observed by immunohistochemical labeling with an antibody for Aβ (4G8, Sigma). In the control (marked by the arrowhead, Figure 2), there was no notable Aβ labeling. The results suggest that these novel ^{125}I-labeled styrylpyridine probes were specifically labeling Aβ plaque sites. Furthermore, ligand [^{125}I]**4**, a well characterized SPECT imaging agent for amyloid plaques,[37] displayed a similar pattern of Aβ plaque labeling using adjacent sections from the macro-array. These results confirmed that the binding of these radioiodinated styrylpyridine probes was specific for Aβ plaques. However, the *N*-methylamino ligands, that is, [^{125}I]**13b** and [^{125}I]**16b**, displayed a less intense and moderate plaque labeling (see Figure

2). This could be due to the labeling conditions, which were not currently optimized for individual ligand. In addition, sections fixed in formalin and subsequently treated with xylene during plaque labeling may lead to some alternation affecting the ligand recognition site(s).

To further characterize the specific nature of plaque binding, we chose [^{125}I]**16b** to carry out a direct in vitro binding assay using AD brain homogenates. As expected, [^{125}I]**16b** displayed highly specific and saturable binding (data not shown). However, there was a large amount of nonspecific filter (glass fiber GF/B) binding in this assay. The nonspecific binding makes this assay an unfavorable tool for quantitatively testing the burden of Aβ plaque in the brain tissue. To solve this problem, we are currently trying different methods to increase the signal detection.

In conclusion, a new series of novel radioiodinated styrylpyridine derivatives, containing a pegylated chain, were successfully prepared as potential SPECT imaging agents for AD. These novel styrylpyridine derivatives displayed excellent binding affinities to Aβ plaques (K_i in the nM range). The radioiodinated probes showed desirable in vivo brain penetration and fast washout in the mouse brain. A specific plaque-labeling signal was clearly indicated for these probes in postmortem AD brain sections as well as in brain tissue homogenates. When labeled with ^{123}I, this novel series of styrylpyridine ligands could be potentially useful for in vivo SPECT imaging of Aβ plaques.

Experimental Section

General Information. All reagents used were commercial products and were used without further purification unless otherwise indicated. All reactions were carried out in flame-dried glassware under nitrogen atmosphere. Flash chromatography (FC) was performed using silica gel 60 (230−400 mesh, Sigma-Aldrich). Preparative thin layer chromatography (PTLC) was performed on silica gel plates with a fluorescent indicator that was visualized with light at 254 nm (Analtech). For each procedure, "standard workup" refers to the following steps: addition of the indicated organic solvent, washing the organic layer with water then brine, separation of the organic layer from the aqueous layer, drying off the combined organic layers with sodium sulfate or magnesium sulfate, filtering off the solid, and concentrating the filtrate under reduced pressure. ^{1}H NMR spectra were obtained at 200 MHz and ^{13}C NMR spectra were recorded at 50 MHz in CDCl$_3$ (Bruker DPX spectrometer). Chemical shifts were reported as δ values (parts per million) relative to internal TMS. Coupling constants were reported in hertz. The multiplicity is defined by s (singlet), d (doublet), t (triplet), br (broad), or m (multiplet). High-resolution MS experiments were performed at the McMaster Regional Centre for Mass Spectrometry using a Micromass/Waters GCT instrument (GC-EI/ CI time-of-flight mass spectrometer). Elemental analyses were performed by Atlantic Microlab Inc. Analytical HPLC analysis was carried out using an Agilent 1100 series LC. Two systems were used to confirm the purity of some compounds listed in this section: system A conditions, Hamilton PRP-1 reverse-phase analytical column (4.1 × 250 mm, 10 μm), 80/20 CH$_3$CN/1 mM ammonium formate (pH = 7) water buffer, 1.0 mL/min, UV 350 nm; system B conditions, Phenomenex silica column (4.6 × 250 mm, 5 μm), 40/60 EtOAc/hexanes, 1.0 mL/min, UV 350 nm. All compounds reported in this paper showed greater than 95% purity in both systems.

3-Bromo-5-iodopyridin-2-ol (8). Following a previously reported method,[45] compound **8** was prepared from *N*-iodosuccinimide (2.48 g, 11.0 mmol) and 3-bromo-2-hydroxypyridine **7** (1.74 g, 10.0 mmol) as a pale brown solid (2.55 g, 85%). ^{1}H NMR (DMSO-d_6) δ 12.27 (br s, 1H), 8.08 (d, 1H, J = 2.3 Hz), 7.71 (d, 1H, J = 2.3 Hz).

3-Bromo-(2-(2-(2-Fluoroethoxy)ethoxy)ethoxy)-5-iodopyridine (9). To a stirring suspension of **8** (0.393 g, 1.3 mmol), 2-(2-

(2-fluoroethoxy)ethoxy)ethanol (0.200 g, 1.3 mmol), and PPh$_3$ (0.511 g,1.95 mmol) in 10 mL of THF at −5 °C was added dropwise diisopropyl azodicarboxylate (DIAD, 0.394 g, 1.95 mmol) in 5 mL of THF. The ice−salt bath was removed, and the reaction was kept at room temperature (rt) for 2 h. The reaction solution was concentrated and purified by FC (MeOH/CHCl$_3$, 1/99) to yield **9**, a colorless viscous liquid (0.423 g, 75%). ^{1}H NMR δ 8.21 (d, 1H, J = 2.0 Hz), 8.02 (d, 1H, J = 2.0 Hz), 4.66 (t, 1H, J = 4.1 Hz), 4.50−4.39 (m, 3H), 3.89−3.64 (m, 8H). ^{13}C NMR δ 159.4, 151.2, 148.5, 108.5, 84.9, 81.6, 81.5, 71.1, 71.0, 70.8, 70.4, 69.3, 66.9. HRMS calcd for C$_{11}$H$_{14}$BrFINO$_3$ (M$^+$), 432.9186; found, 432.9173.

2-(3-Bromo-5-iodopyridin-2-yloxy)ethanol (10). To a stirring suspension of **8** (0.906 g, 3.0 mmol), 2-(*tert*-butyl-dimethylsilanyloxy)ethanol (0.554 g, 3.15 mmol), and PPh$_3$ (0.944 g, 3.6 mmol) in 20 mL of THF at −5 °C was added dropwise diisopropylazodicarboxylate (DIAD, 0.728 g, 3.6 mmol) in 10 mL of THF. The ice−salt bath was removed, and the reaction was kept at rt for 2 h. The reaction solution was concentrated and purified by FC (EtOAc/hexanes, 5/95) to afford **3-bromo-2-(2-(*tert*-butyl-dimethylsilyloxy)ethoxy)-5-iodopyridine**, a colorless viscous liquid (0.995 g, 72%). ^{1}H NMR δ 8.23 (d, 1H, J = 2.0 Hz), 8.05 (d, 1H, J = 2.0 Hz), 4.42 (t, 2H, J = 4.9 Hz), 3.98 (t, 2H, J = 4.9 Hz), 0.90 (s, 9H), 0.10 (s, 6H). HRMS calcd for C$_{12}$H$_{18}$BrINO$_2$Si (M − CH$_3$$^+$), 441.9335; found, 441.9312.

3-Bromo-2-(2-(*tert*-butyl-dimethylsilyloxy)ethoxy)-5-iodopyridine (0.230 g, 0.50 mmol) was added to 5 mL of 95% EtOH containing 1% concd HCl and stirred at rt for 0.5 h. The reaction solution was poured into 20 mL of ice-cold 5% Na$_2$CO$_3$, and the aqueous layer was extracted with CH$_2$Cl$_2$ (15 mL × 3). The organic layers were collected, dried, filtered, and concentrated. The residue was purified by FC (EtOAc/hexanes, 30/70) and afforded **10** as a white solid (0.169 g, 94%). ^{1}H NMR δ 8.24 (d, 1H, J = 2.0 Hz), 8.09 (d, 1H, J = 2.0 Hz), 4.50 (t, 2H, J = 4.5 Hz), 4.02−3.93 (m, 2H), 2.58−2.52 (m, 1H, −OH). ^{13}C NMR δ 159.5, 151.2, 148.9, 108.7, 81.9, 69.6, 61.7. HRMS calcd for C$_7$H$_7$BrINO$_2$ (M$^+$), 342.8705; found, 342.8707.

General Procedure of the Heck Reaction for the Synthesis of Bromo-Substituted Styryl-Pyridine Derivatives (11a−d, 14a,b, and 14d). (*E*)-4-(2-(5-Bromo-6-(2-(2-(2-fluoroethoxy)-ethoxy)ethoxy)pyridin-3-yl)vinyl)-*N,N*-dimethylbenzenamine (11a). A mixture of 4-dimethylaminostyrene (0.110 g, 0.75 mmol), **9** (0.217 g, 0.5 mmol), K$_2$CO$_3$ (0.173 g, 1.25 mmol), tetrabutylammonium bromide (TBAB, 0.322 g, 1.0 mmol), and palladium acetate (Pd(OAc)$_2$, 0.006 g, 0.025 mmol) in 2 mL of DMF was deoxygenated by purging into nitrogen for 15 min and then heating to 65 °C for 2 h. The reaction mixture was cooled to rt and submitted to standard workup with ethyl acetate (EtOAc). The crude product was purified by FC (EtOAc/hexanes, 30/70) and resulted in **11a** as a light yellow solid (0.178 g, 79%). ^{1}H NMR δ 8.08 (d, 1H, J = 2.1 Hz), 8.00 (d, 1H, J = 2.1 Hz), 7.39 (d, 2H, J = 8.8 Hz), 6.92 (d, 1H, J = 16.3 Hz), 6.74 (d, 1H, J = 16.3 Hz), 6.72 (d, 2H, J = 8.1 Hz), 4.69 (t, 1H, J = 4.2 Hz), 4.55 (t, 2H, J = 4.8 Hz), 4.45 (t, 1H, J = 4.2 Hz), 3.94−3.68 (m, 8H), 3.00 (s, 6H). ^{13}C NMR δ 158.3, 150.4, 143.5, 138.0, 129.6, 129.5, 127.7, 125.2, 118.8, 112.5, 107.5, 85.0, 81.6, 71.2, 71.0, 70.8, 70.4, 69.6, 66.7, 40.5. HRMS calcd for C$_{21}$H$_{26}$BrFN$_2$O$_3$ (M$^+$), 452.1111; found, 452.1099.

(*E*)-4-(2-(5-Bromo-6-(2-(2-(2-fluoroethoxy)ethoxy)ethoxy)pyridin-3-yl)vinyl)-*N*-methylbenzenamine (11b). Compound **11b** was prepared from 4-methylaminostyrene (0.073 g, 0.55 mmol) and **9** (0.217 g, 0.50 mmol) as a light yellow viscous liquid (0.113 g, 52% yield). ^{1}H NMR δ 8.07 (d, 1H, J = 2.1 Hz), 8.00 (d, 1H, J = 2.1 Hz), 7.35 (d, 2H, J = 8.6 Hz), 6.91 (d, 1H, J = 16.3 Hz), 6.74 (d, 1H, J = 16.3 Hz), 6.60 (d, 2H, J = 8.6 Hz), 4.69 (t, 1H, J = 4.2 Hz), 4.55 (t, 2H, J = 4.8 Hz), 4.45 (t, 1H, J = 4.2 Hz), 3.94−3.68 (m, 8H), 2.88 (s, 3H). ^{13}C NMR δ 158.4, 149.5, 143.6, 138.0, 129.8, 129.5, 127.9, 126.1, 118.9, 112.6, 107.5, 85.0, 81.7, 71.2, 71.1, 70.8, 70.4, 69.6, 66.8, 30.7. HRMS calcd for C$_{20}$H$_{24}$BrFN$_2$O$_3$ (M$^+$), 438.0954; found, 438.0967.

(*E*)-*tert*-Butyl 4-(2-(5-Bromo-6-(2-(2-(2-fluoroethoxy)ethoxy)-ethoxy)pyridin-3-yl)vinyl)phenyl(methyl)carbamate (11c). Com-

pound **11c** was prepared from 4-*N*-methyl-4-*N*-(tert-butyloxycarbonyl)aminostyrene (0.219 g, 0.94 mmol) and **9** (0.273 g, 0.63 mmol) as a white viscous liquid (0.319 g, 94% yield). ^{1}H NMR δ 8.12 (d, 1H, $J = 2.1$ Hz), 8.03 (d, 1H, $J = 2.1$ Hz), 7.44 (d, 2H, $J = 8.6$ Hz), 7.25 (d, 2H, $J = 9.0$ Hz), 6.94 (d, 2H, $J = 2.1$ Hz), 4.69 (t, 1H, $J = 4.2$ Hz), 4.56 (t, 2H, $J = 4.9$ Hz), 4.45 (t, 1H, $J = 4.2$ Hz), 3.94–3.68 (m, 8H), 3.28 (s, 3H), 1.48 (s, 9H). ^{13}C NMR δ 158.8, 154.5, 144.0, 143.5, 138.2, 133.6, 128.5, 128.4, 126.8, 126.6, 125.4, 122.9, 107.4, 84.8, 81.4, 80.4, 71.0, 70.9, 70.6, 70.2, 69.4, 66.7, 53.5, 37.1, 28.4. HRMS calcd for $C_{25}H_{32}BrFN_2O_5$ (M$^+$), 538.1479; found, 538.1476.

(*E*)-4-(2-(5-Bromo-6-(2-(2-(2-fluoroethoxy)ethoxy)ethoxy)pyridin-3-yl)vinyl)phenyl Acetate (11d). Compound **11d** was prepared from 4-acetoxystyrene (0.122 g, 0.75 mmol) and **9** (0.217 g, 0.5 mmol) as a white viscous liquid (0.181 g, 77% yield). ^{1}H NMR δ 8.12 (d, 1H, $J = 2.1$ Hz), 8.03 (d, 1H, $J = 2.1$ Hz), 7.50 (d, 2H, $J = 8.6$ Hz), 7.10 (d, 2H, $J = 8.6$ Hz), 6.94 (d, 2H, $J = 3.3$ Hz), 4.69 (t, 1H, $J = 4.2$ Hz), 4.56 (t, 2H, $J = 4.9$ Hz), 4.45 (t, 1H, $J = 4.2$ Hz), 3.94–3.68 (m, 8H), 2.32 (s, 3H), 1.48 (s, 9H). ^{13}C NMR δ 169.3, 158.9, 150.3, 144.1, 138.2, 134.5, 128.24, 128.16, 127.4, 123.4, 121.9, 107.5, 84.8, 81.5, 71.0, 70.9, 70.6, 70.3, 69.4, 66.7, 21.1. HRMS calcd for $C_{21}H_{23}BrFNO_5$ (M$^+$), 467.0744; found, 467.0731.

(*E*)-2-(3-Bromo-5-(4-(dimethylamino)styryl)pyridin-2-yloxy)ethanol (14a). Compound **14a** was prepared from 4-dimethylaminostyrene (0.031 g, 0.212 mmol) and **10** (0.073 g, 0.212 mmol) as a light yellow solid (0.022 g, 29% yield). ^{1}H NMR δ 8.07 (d, 1H, $J = 2.1$ Hz), 8.03 (d, 1H, $J = 2.1$ Hz), 7.39 (d, 2H, $J = 8.8$ Hz), 6.94 (d, 1H, $J = 16.3$ Hz), 6.78–6.69 (m, 3H), 4.57–4.52 (m, 2H), 3.99 (t, 2H, $J = 4.3$ Hz), 3.21 (br s, 1H), 3.00 (s, 6H). ^{13}C NMR δ 158.3, 150.4, 143.0, 138.2, 129.9, 129.8, 127.6, 124.9, 118.3, 112.3, 107.5, 69.6, 62.1, 40.3. HRMS calcd for $C_{17}H_{19}BrN_2O_2$ (M$^+$), 362.063; found, 362.0629.

(*E*)-2-(3-Bromo-5-(4-(methylamino)styryl)pyridin-2-yloxy)ethanol (14b). Compound **14b** was prepared from 4-methylaminostyrene (0.140 g, 1.05 mmol) and **10** (0.241 g, 0.7 mmol) as a light yellow viscous liquid (0.149 g, 61% yield). ^{1}H NMR δ 8.07 (d, 1H, $J = 2.1$ Hz), 8.03 (d, 1H, $J = 2.1$ Hz), 7.35 (d, 2H, $J = 8.6$ Hz), 6.93 (d, 1H, $J = 16.3$ Hz), 6.74 (d, 1H, $J = 16.3$ Hz), 6.61 (d, 2H, $J = 8.6$ Hz), 4.57–4.52 (m, 2H), 3.99 (br s, 2H), 3.18 (br s, 1H), 2.88 (s, 3H). ^{13}C NMR δ 149.6, 143.3, 138.5, 130.1, 130.0, 128.0, 126.0, 118.6, 112.6, 107.7, 69.8, 62.2, 30.7. HRMS calcd for $C_{17}H_{19}BrN_2O_2$ (M$^+$), 348.0473; found, 348.0468.

(*E*)-4-(2-(5-Bromo-6-(2-hydroxyethoxy)pyridin-3-yl)vinyl)phenyl Acetate (14d). Compound **14d** was prepared from 4-acetoxystyrene (0.130 g, 0.80 mmol) and **10** (0.244 g, 0.7 mmol) as a white viscous liquid (0.031 g, 12% yield). ^{1}H NMR δ 8.12 (d, 1H, $J = 2.1$ Hz), 8.08 (d, 1H, $J = 2.1$ Hz), 7.50 (d, 2H, $J = 6.8$ Hz), 7.11 (d, 2H, $J = 6.8$ Hz), 6.95 (d, 2H, $J = 5.2$ Hz), 4.58–4.54 (m, 2H), 4.01 (br s, 2H), 3.08 (br s, 1H), 2.32 (s, 3H).

(*E*)-4-(2-(5-Bromo-6-(2-(2-(2-fluoroethoxy)ethoxy)ethoxy)pyridin-3-yl)vinyl)phenol (11e). Acetate **11d** (0.145 g, 0.31 mmol) and K$_2$CO$_3$ (0.064 g, 0.465 mmol) were placed in EtOH/THF (5 mL/5 mL), and the reaction mixture was stirred at rt for 2 h. After standard workup with EtOAc, the crude product was purified by PTLC to give **11e** as a white solid (0.128 g, 97%). ^{1}H NMR δ 8.07 (d, 1H, $J = 2.1$ Hz), 7.99 (d, 1H, $J = 2.1$ Hz), 7.35 (d, 2H, $J = 8.6$ Hz), 6.96–6.74 (m, 4H), 5.22 (br s, 1H), 4.69 (t, 1H, $J = 4.2$ Hz), 4.54 (t, 2H, $J = 4.8$ Hz), 4.45 (t, 1H, $J = 4.2$ Hz), 3.94–3.68 (m, 8H). ^{13}C NMR δ 158.5, 156.4, 143.6, 138.2, 129.2, 129.0, 127.9, 120.7, 116.0, 107.6, 84.9, 81.6, 71.1, 71.0, 70.8, 70.4, 69.6, 66.8. HRMS calcd for $C_{19}H_{21}BrFNO_4$ (M$^+$), 425.0638; found, 425.0651.

(*E*)-4-(2-(5-Bromo-6-(2-hydroxyethoxy)pyridin-3-yl)vinyl)phenol (14e). In a similar procedure as described in the preparation of **11e**, compound **14e** was prepared from acetate **14d** (0.031 g, 0.082 mmol) as a white solid (0.020 g, 73%). ^{1}H NMR (DMSO-*d*$_6$) δ 9.60 (br s, 1H), 8.31 (s, 1H), 8.23 (s, 1H), 7.39 (d, 2H, $J = 8.3$ Hz), 7.19 (d, 1H, $J = 16.8$ Hz), 6.94 (d, 1H, $J = 16.6$ Hz), 6.77 (d, 2H, $J = 8.3$ Hz), 4.35 (t, 2H, $J = 5.1$ Hz), 3.73 (t, 2H, $J = 5.1$ Hz). ^{13}C NMR (DMSO-*d*$_6$) δ 157.9, 157.4, 143.7, 138.1,

129.2, 129.0, 127.8, 119.8, 115.6, 106.7, 68.4, 59.2. HRMS calcd for $C_{15}H_{14}BrNO_3$ (M$^+$), 335.0157; found, 335.0165.

General Procedure of the Stannylation for the Synthesis of Tributyltin-Substituted Styryl-Pyridine Derivatives (12a–c, 12e, and 15a,b, 15e). **(*E*)-4-(2-(6-(2-(2-(2-Fluoroethoxy)ethoxy)ethoxy)-5-(tributylstannyl)pyridin-3-yl)vinyl)-*N*,*N*-dimethylbenzenamine (12a).** A mixture of **11a** (0.052 g, 0.115 mmol), bis-(tributyltin) ((Bu$_3$Sn)$_2$, 0.333 g, 0.57 mmol), and palladium tetrakistriphenylphosphine (Pd(PPh$_3$)$_4$, 0.013 g, 10 mol %) in toluene was heated at 110 °C for 18 h. The reaction solution was cooled to rt and treated with 5 mL of 10% KF. After vigorously stirring for an additional 0.5 h, the standard workup with EtOAc and the following FC (EtOAc/hexanes, 25/75) afforded **12a** as a light yellow oil (0.052 g, 68%). ^{1}H NMR δ 8.11 (d, 1H, $J = 2.5$ Hz), 7.81 (d, 1H, $J = 2.5$ Hz), 7.41 (d, 2H, $J = 8.8$ Hz), 6.93 (d, 1H, $J = 16.5$ Hz), 6.81 (d, 1H, $J = 16.5$ Hz), 6.72 (d, 2H, $J = 8.7$ Hz), 4.69 (t, 1H, $J = 4.2$ Hz), 4.46 (t, 3H, $J = 4.9$ Hz), 3.83 (t, 3H, $J = 4.8$ Hz), 3.71–3.66 (m, 5H), 3.00 (s, 6H), 1.68–1.48 (m, 6H), 1.43–1.21 (m, 6H), 1.15–1.02 (m, 6H), 0.91 (t, 9H, $J = 7.1$ Hz). ^{13}C NMR δ 166.7, 150.2, 145.4, 143.6, 127.8, 127.7, 127.5, 126.0, 123.7, 121.2, 112.6, 85.0, 81.6, 71.0, 70.8, 70.7, 70.4, 70.0, 65.0, 40.6, 29.5, 29.3, 29.1, 28.1, 27.5, 26.9, 13.9, 13.4, 13.3, 9.9, 6.6, 6.4. HRMS calcd for $C_{33}H_{53}FN_2O_3Sn$ (M$^+$), 664.3062; found, 664.3037.

(*E*)-4-(2-(6-(2-(2-(2-Fluoroethoxy)ethoxy)ethoxy)-5-(tributylstannyl)pyridin-3-yl)vinyl)-*N*-methylbenzenamine (12b). Compound **12b** was prepared from **11b** (0.069 g, 0.156 mmol) as a light yellow oil (0.068 g, 68% yield). ^{1}H NMR δ 8.10 (d, 1H, $J = 2.5$ Hz), 7.80 (d, 1H, $J = 2.5$ Hz), 7.36 (d, 2H, $J = 8.6$ Hz), 6.92 (d, 1H, $J = 16.3$ Hz), 6.80 (d, 1H, $J = 16.3$ Hz), 6.61 (d, 2H, $J = 8.6$ Hz), 4.69 (t, 1H, $J = 4.2$ Hz), 4.45 (t, 3H, $J = 5.1$ Hz), 3.83 (t, 3H, $J = 4.4$ Hz), 3.71–3.66 (m, 5H), 2.88 (s, 3H), 1.68–1.48 (m, 6H), 1.43–1.25 (m, 6H), 1.15–1.02 (m, 6H), 0.91 (t, 9H, $J = 7.1$ Hz). ^{13}C NMR δ 166.8, 149.1, 145.4, 143.6, 127.8, 127.7, 127.0, 123.8, 121.2, 112.6, 85.0, 81.6, 71.1, 70.9, 70.8, 70.5, 70.1, 65.0, 30.8, 29.5, 29.3, 29.1, 28.1, 27.5, 26.9, 13.9, 13.4, 13.3, 9.9, 6.6, 6.4. HRMS calcd for $C_{32}H_{51}FN_2O_3Sn$ (M$^+$), 650.2906; found, 650.2894.

(*E*)-*tert*-Butyl 4-(2-(6-(2-(2-(2-Fluoroethoxy)ethoxy)ethoxy)-5-(tributylstannyl)pyridin-3-yl)vinyl)phenyl(methyl)carbamate (12c). Compound **12c** was prepared from **11c** (0.072 g, 0.133 mmol) as a white viscous liquid (0.077 g, 77% yield). ^{1}H NMR δ 8.14 (d, 1H, $J = 2.5$ Hz), 7.83 (d, 1H, $J = 2.5$ Hz), 7.46 (d, 2H, $J = 8.6$ Hz), 7.23 (d, 2H, $J = 8.5$ Hz), 6.96 (s, 2H), 4.70–4.66 (m, 1H), 4.49–4.42 (m, 3H), 3.86–3.66 (m, 8H), 3.28 (s, 3H), 1.80–1.02 (m, 27H), 0.90 (t, 9H, $J = 7.1$ Hz). ^{13}C NMR δ 167.3, 146.1, 143.8, 143.2, 134.6, 127.0, 126.8, 126.6, 125.7, 125.4, 124.1, 85.0, 81.6, 80.6, 71.1, 70.9, 70.8, 70.5, 70.0, 65.1, 37.4, 29.5, 29.3, 29.1, 28.1, 27.5, 26.9, 13.9, 13.4, 9.9, 6.4. HRMS calcd for $C_{37}H_{59}FN_2O_5Sn$ (M$^+$), 750.343; found, 750.3425.

(*E*)-4-(2-(6-(2-(2-(2-Fluoroethoxy)ethoxy)ethoxy)-5-(tributylstannyl)pyridin-3-yl)vinyl)phenol (12e). Compound **12e** was prepared from **11e** (0.032 g, 0.075 mmol) as a white viscous liquid (0.040 g, 84% yield). ^{1}H NMR δ 8.11 (d, 1H, $J = 2.5$ Hz), 7.82 (d, 1H, $J = 2.5$ Hz), 7.39 (d, 2H, $J = 8.6$ Hz), 6.98–6.74 (m, 4H), 5.19 (br s, 1H), 4.71–4.66 (m, 1H), 4.48–4.43 (m, 3H), 3.90–3.62 (m, 8H), 1.70–1.02 (m, 18H), 0.91 (t, 9H, $J = 7.1$ Hz). ^{13}C NMR δ 166.9, 156.0, 145.4, 144.0, 130.1, 127.9, 127.6, 127.4, 124.3, 123.0, 115.9, 85.0, 81.6, 71.0, 70.9, 70.7, 70.5, 70.0, 65.2, 29.5, 29.3, 29.1, 28.0, 27.5, 26.9, 13.9, 13.4, 13.3, 9.9, 6.6, 6.4. HRMS calcd for $C_{31}H_{48}FNO_4Sn$ (M$^+$), 637.2589; found, 637.2573.

(*E*)-2-(5-(4-(Dimethylamino)styryl)-3-(tributylstannyl)-pyridin-2-yloxy)ethanol (15a). Compound **15a** was prepared from **14a** (0.100 g, 0.275 mmol) as a light yellow oil (0.105 g, 66% yield). ^{1}H NMR δ 8.10 (d, 1H, $J = 2.5$ Hz), 7.85 (d, 1H, $J = 2.4$ Hz), 7.41 (d, 2H, $J = 8.7$ Hz), 6.95 (d, 1H, $J = 16.3$ Hz), 6.81 (d, 1H, $J = 16.6$ Hz), 6.73 (d, 2H, $J = 8.8$ Hz), 4.48–4.44 (m, 2H), 3.96–3.92 (m, 2H), 2.99 (s, 6H), 1.68–1.01 (m, 18H), 0.92 (t, 9H, $J = 7.2$ Hz). ^{13}C NMR δ 166.6, 150.1, 144.5, 144.1, 128.2, 128.1, 127.4, 125.6, 124.0, 120.5, 112.4, 69.4, 63.0, 40.4, 29.0, 27.2, 13.6, 9.8. HRMS calcd for $C_{29}H_{46}N_2O_2Sn$ (M$^+$), 574.2581; found, 574.2584.

(*E*)-2-(5-(4-(Methylamino)styryl)-3-(tributylstannyl)-pyridin-2-yloxy)ethanol (15b). Compound **15b** was prepared from **14b** (0.052 g, 0.15 mmol) as a light yellow oil (0.059 g, 64% yield). ^{1}H NMR δ 8.08 (d, 1H, $J = 2.5$ Hz), 7.84 (d, 1H, $J = 2.4$ Hz), 7.37 (d, 2H, $J = 8.6$ Hz), 6.93 (d, 1H, $J = 16.3$ Hz), 6.80 (d, 1H, $J = 16.4$ Hz), 6.61 (d, 2H, $J = 8.6$ Hz), 4.48–4.43 (m, 2H), 3.95–3.91 (m, 2H), 2.88 (s, 3H), 1.69–1.01 (m, 18H), 0.91 (t, 9H, $J = 7.1$ Hz). ^{13}C NMR δ 166.9, 149.2, 144.7, 144.3, 128.4, 128.3, 127.8, 126.7, 124.2, 120.7, 112.6, 69.6, 63.2, 30.8, 29.5, 29.3, 29.1, 28.0, 27.5, 26.9, 13.9, 13.5, 13.4, 10.0, 6.6, 6.5. HRMS calcd for $C_{28}H_{44}N_2O_2Sn$ (M$^+$), 560.2425; found, 560.2419.

(*E*)-4-(2-(6-(2-Hydroxyethoxy)-5-(tributylstannyl)-pyridin-3-yl)vinyl)phenol (15e). Compound **15e** was prepared from **14e** (0.031 g, 0.092 mmol) as a white viscous liquid (0.012 g, 24% yield). ^{1}H NMR δ 8.07 (d, 1H, $J = 2.5$ Hz), 7.85 (d, 1H, $J = 2.5$ Hz), 7.39 (d, 2H, $J = 8.6$ Hz), 6.99–6.80 (m, 4H), 5.97 (br s, 1H), 5.01 (br s, 1H), 4.50–4.46 (m, 2H), 3.98–3.94 (m, 2H), 1.69–1.01 (m, 18H), 0.91 (t, 9H, $J = 7.1$ Hz). ^{13}C NMR δ 167.2, 156.0, 144.9, 144.7, 144.5, 130.1, 128.0, 127.96, 124.7, 122.8, 116.0, 69.9, 63.4, 29.9, 29.5, 29.3, 29.1, 28.1, 27.5, 26.9, 13.9, 13.6, 13.5, 10.1, 6.7, 6.6. HRMS calcd for $C_{27}H_{41}NO_3Sn$ (M$^+$), 547.2108; found, 547.2112.

General Procedure of the Iodo-Tributyltin Exchange Reaction for the Synthesis of Iodo-Substituted Styryl-Pyridine Derivatives (13a, 13c, 13e and 16a,b, 16e). **(*E*)-4-(2-(6-(2-(2-(2-Fluoroethoxy)ethoxy)ethoxy)-5-iodopyridin-3-yl)vinyl)-*N,N*-dimethylbenzenamine (13a).** A solution of iodine (I$_2$, 0.063 g, 0.24 mmol) in THF (2 mL) was added dropwise to an ice bath cooled solution of **12a** (0.114 g, 0.172 mmol) in THF (3 mL). After the addition, the reaction was stirred at 0 °C for 1 h. Following standard workup with CH$_2$Cl$_2$, the crude product was purified by FC (EtOAc/hexanes, 25/75) to give a light yellow solid **13a** (0.037 g, 48%). ^{1}H NMR δ 8.22 (d, 1H, $J = 2.1$ Hz), 8.10 (d, 1H, $J = 2.1$ Hz), 7.38 (d, 2H, $J = 8.8$ Hz), 6.92 (d, 1H, $J = 16.3$ Hz), 6.72 (d, 1H, $J = 16.3$ Hz), 6.71 (d, 2H, $J = 8.8$ Hz), 4.72–4.67 (m, 1H), 4.54–4.44 (m, 3H), 3.93–3.69 (m, 8H), 3.00 (s, 6H). ^{13}C NMR δ 160.4, 150.5, 144.6, 144.55, 129.8, 129.5, 127.8, 125.3, 118.8, 112.6, 85.1, 81.7, 80.6, 71.3, 71.1, 70.8, 70.5, 69.6, 67.1, 40.6. HRMS calcd for $C_{21}H_{26}FIN_2O_3$ (M$^+$), 500.0972; found, 500.0959.

(*E*)-*tert*-Butyl 4-(2-(6-(2-(2-(2-Fluoroethoxy)ethoxy)ethoxy)-5-iodopyridin-3-yl)vinyl)phenyl(methyl)carbamate (13c). Compound **13c** was prepared from **12c** (0.024 g, 0.032 mmol) as a white viscous liquid (0.018 g, 98%). ^{1}H NMR δ 8.25 (d, 1H, $J = 1.6$ Hz), 8.13 (d, 1H, $J = 1.6$ Hz), 7.44 (d, 2H, $J = 8.4$ Hz), 7.24 (d, 2H, $J = 8.4$ Hz), 6.97 (d, 1H, $J = 16.4$ Hz), 6.86 (d, 1H, $J = 16.4$ Hz), 4.69 (t, 1H, $J = 4.1$ Hz), 4.53 (t, 2H, $J = 4.8$ Hz), 4.45 (t, 1H, $J = 4.1$ Hz), 3.94–3.69 (m, 8H), 3.28 (s, 3H), 1.47 (s, 9H). ^{13}C NMR δ 161.0, 154.8, 145.3, 144.9, 143.7, 133.9, 128.9, 128.6, 126.8, 125.7, 123.1, 85.1, 81.7, 80.7, 77.4, 71.3, 71.1, 70.9, 70.5, 69.6, 67.2, 37.4, 28.6. HRMS calcd for $C_{21}H_{26}FIN_2O_3$ (M$^+$), 500.0972; found, 500.0959.

(*E*)-4-(2-(6-(2-(2-(2-Fluoroethoxy)ethoxy)ethoxy)-5-iodopyridin-3-yl)vinyl)phenol (13e). Compound **13e** was prepared from **12e** (0.012 g, 0.019 mmol) as a white solid (0.008 g, 90%). ^{1}H NMR δ 8.21 (d, 1H, $J = 2.1$ Hz), 8.08 (d, 1H, $J = 2.1$ Hz), 7.33 (d, 2H, $J = 8.6$ Hz), 6.94–6.69 (m, 4H), 4.71–4.67 (m, 1H), 4.53–4.43 (m, 3H), 3.94–3.69 (m, 8H). HRMS calcd for $C_{19}H_{21}FINO_4$ (M$^+$), 473.0499; found, 473.0498.

(*E*)-2-(5-(4-(Dimethylamino)styryl)-3-iodopyridin-2-yloxy)-ethanol (16a). Compound **16a** was prepared from **15a** (0.011 g, 0.019 mmol) as a light yellow solid (0.004 g, 50%). ^{1}H NMR δ 8.25 (s, 1H), 8.10 (s, 1H), 7.39 (d, 2H, $J = 8.6$ Hz), 6.94 (d, 1H, $J = 16.3$ Hz), 6.76–6.70 (m, 3H), 4.51 (t, 2H, $J = 4.2$ Hz), 4.02–3.95 (m, 2H), 3.19 (s, 1H), 3.00 (s, 6H). HRMS calcd for $C_{17}H_{19}IN_2O_2$ (M$^+$), 410.0491; found, 410.0489.

(*E*)-2-(3-Iodo-5-(4-(methylamino)styryl)pyridin-2-yloxy)etha-nol (16b). Compound **16b** was prepared from **15b** (0.032 g, 0.057 mmol) as a light yellow solid (0.005 g, 21%). ^{1}H NMR δ 8.24 (d, 1H, $J = 2.1$ Hz), 8.09 (d, 1H, $J = 2.0$ Hz), 7.36 (d, 2H, $J = 8.5$ Hz), 6.92 (d, 1H, $J = 16.3$ Hz), 6.76–6.64 (m, 3H), 4.53–4.49

(m, 2H), 4.01–3.96 (m, 2H), 2.96 (s, 1H), 2.89 (s, 3H). HRMS calcd for $C_{16}H_{17}IN_2O_2$ (M$^+$), 396.0335; found, 396.0335.

(*E*)-4-(2-(6-(2-Hydroxyethoxy)-5-iodopyridin-3-yl)vinyl)phe-nol (16e). Compound **16e** was prepared from **15e** (0.009 g, 0.017 mmol) as a white solid (0.003 g, 50%). ^{1}H NMR δ 8.26 (d, 1H, $J = 2.1$ Hz), 8.10 (d, 1H, $J = 2.1$ Hz), 7.38 (d, 2H, $J = 8.6$ Hz), 6.98–6.73 (m, 4H), 4.55–4.47 (m, 2H), 4.02–3.98 (m, 2H), 3.25 (br s, 1H). HRMS calcd for $C_{16}H_{17}IN_2O_2$ (M$^+$), 383.0018; found, 383.0022.

(*E*)-4-(2-(6-(2-(2-(2-Fluoroethoxy)ethoxy)ethoxy)-5-iodopyri-din-3-yl)vinyl)-N-methylbenzenamine (13b). To a stirred solution of **13c** (0.014 g, 0.024 mmol) and 2,6-lutidine (28 μL, 0.24 mmol) in 2 mL of CH$_2$Cl$_2$ at 0 °C was added trimethylsilyl triflate (34 μL, 0.19 mmol). After 15 min, the reaction solution was submitted to the standard workup with CH$_2$Cl$_2$. The crude product was purified by PTLC to give a light yellow viscous liquid **13b** (0.010 g, 88%). ^{1}H NMR δ 8.22 (d, 1H, $J = 2.1$ Hz), 8.10 (d, 1H, $J = 2.1$ Hz), 7.34 (d, 2H, $J = 8.6$ Hz), 6.91 (d, 1H, $J = 16.3$ Hz), 6.70 (d, 1H, $J = 16.3$ Hz), 6.60 (d, 2H, $J = 8.6$ Hz), 4.71–4.67 (m, 1H), 4.54–4.43 (m, 3H), 3.94–3.69 (m, 9H), 2.88 (s, 3H). ^{13}C NMR δ 160.5, 149.5, 144.6, 129.8, 129.7, 128.0, 126.3, 118.9, 112.6, 85.1, 81.7, 80.6, 77.4, 71.3, 71.2, 70.9, 70.5, 69.7, 67.2, 30.8. HRMS calcd for $C_{20}H_{24}FIN_2O_3$ (M$^+$), 486.0816; found, 486.0818.

Radioiodination. Radioiodinated compounds, [^{125}I]**13a**, **13b**, **16a**, **16b**, and **16e**, were prepared via iododestannylation reactions from the corresponding tributyltin precursors according to the method described previously.[38,56] Hydrogen peroxide (50 μL, 3% w/v) was added to a mixture of 50 μL of the tributyltin precursor (4 μg/μL EtOH), 50 μL of 1 N HCl, and [^{125}I]NaI (1–5 mCi purchased from Perkin-Elmer) in a sealed vial. The reaction was allowed to proceed for 5–10 min at rt and terminated by addition of 100 μL of satd NaHSO$_3$. The reaction mixture was extracted with ethyl acetate (3 × 1 mL) after neutralization with 1.5 mL of satd sodium bicarbonate solution. The combined extracts were evaporated to dryness. The residues were dissolved in 100 μL of EtOH and purified by HPLC using a reversed-phase column (Phenomenex Gemini C18 analytical column , 4.6 × 250 mm, 5 mm, CH$_3$CN/ammonium formate buffer (1 mM) 8/2 or 7/3; flow rate 0.5–1.0 mL/min). The no-carrier-added products were evaporated to dryness and redissolved in 100% EtOH (1 μCi/μL) to be stored at -20 °C up to 6 weeks for animal studies and autoradiography studies.

Preparation of Brain Tissue Homogenates. AD postmortem brain tissues were obtained from University of Washington Alzheimer's Disease Research Center. The neuropathological diagnosis was confirmed by current criteria (NIA-Reagan Institute Consensus Group, 1997). Homogenates were then prepared from dissected gray matters from four pooled AD patients in phosphate buffered saline (PBS, pH 7.4) at the concentration of approximately 100 mg wet tissue/mL (motor-driven glass homogenizer with setting of 6 for 30 s). The homogenates were aliquoted into 1 mL portions and stored at -70 °C for up to 2 years without loss of binding signal.

Binding Studies. Ligand [^{125}I]**4** with 2200 Ci/mmol specific activity and greater than 95% radiochemical purity was prepared using the standard iododestannylation reaction and purified by a simplified C-4 mini-column, as described previously.[38] Competition binding assays were carried out in 12 × 75 mm borosilicate glass tubes. The reaction mixture contained 50 mL of pooled AD brain homogenates (20–50 mg), 50 mL of [^{125}I]**4** (0.04–0.06 nM diluted in PBS), and 50 mL of inhibitors (10^{-5}–10^{-10} M diluted serially in PBS containing 0.1% bovine serum albumin) in a final volume of 1 mL. Nonspecific binding was defined in the presence of 600 nM **4** in the same assay tubes. The mixture was incubated at 37 °C for 2 h and the bound and the free radioactivity were separated by vacuum filtration through Whatman GF/B filters using a Brandel M-24R cell harvester followed by 2 × 3 mL washes of PBS at rt. Filters containing the bound ^{125}I ligand were counted in a gamma counter (Packard 5000) with 70% counting efficiency. Under the assay conditions, the non-specifically bound fraction was less than 15% of the total radioactivity. The results of inhibition experiments

were subjected to nonlinear regression analysis using equilibrium binding data analysis which K_i values were calculated.

In Vitro Autoradiography. To compare different probes using similar sections of human brain tissue, human macro-array brain sections from six confirmed AD cases and one control subject were assembled. The presence and localization of plaques on the sections was confirmed with immunohistochemical staining with monoclonal Aβ antibody 4G8 (Sigma). The sections were incubated with [^{125}I]-tracers (200 000−250 000 cpm/200 mL) for 1 h at rt. The sections were then dipped in satd lithium carbonate in 40% EtOH (two 2 min washes) and washed with 40% EtOH (one 2 min wash), followed by rinsing with water for 30 s. After drying, the ^{125}I-labeled sections were exposed to Kodak Biomax MR film overnight.

Organ Distribution in Normal Mice. While under isoflurane anesthesia, 0.15 mL of a 0.1% bovine serum albumin solution containing [^{125}I]tracers (5−10 μCi) was injected directly into the tail vein of ICR mice (22−25 g, male). The mice ($n = 3$ for each time point) were sacrificed by cervical dislocation at designated time points postinjection. The organs of interest were removed and weighed, and the radioactivity was counted with an automatic gamma counter. The percentage dose per organ was calculated by a comparison of the tissue counts to suitably diluted aliquots of the injected material. The total activity of the blood was calculated under the assumption that it is 7% of the total body weight. The % dose/g of samples was calculated by comparing the sample counts with the count of the diluted initial dose.

Partition Coefficient. Partition coefficients were measured by mixing the [^{125}I]tracer with 3 g each of 1-octanol and buffer (0.1 M phosphate, pH 7.4) in a test tube. The test tube was vortexed for 3 min at rt, followed by centrifugation for 5 min. Two weighed samples (0.5 g each) from the 1-octanol and buffer layers were counted in a well counter. The partition coefficient was determined by calculating the ratio of cpm/g of 1-octanol to that of buffer. Samples from the 1-octanol layer were repartitioned until consistent partitions of coefficient values were obtained. The measurement was done in triplicate and repeated three times.

Supporting Information Available: The procedures for synthesizing some intermediates, elemental analysis results for some bromo-, tributyltin-, and iodo-substituted styryl-pyridine derivatives, and HPLC purity analysis data for all bio-assay involved compounds in two different HPLC systems. This material is available free of charge via the Internet at http://pubs.acs.org.

References

(1) Tsuboi, Y. Neuropathology of familial tauopathy. *Neuropathology* **2006**, *26*, 471−474.

(2) Roberson, E. D.; Mucke, L. 100 years and counting: Prospects for defeating Alzheimer's disease. *Science* **2006**, *314*, 781−784.

(3) Goedert, M.; Spillantini, M. G. A century of Alzheimer's disease. *Science* **2006**, *314*, 777−781.

(4) Hasegawa, M. Biochemistry and molecular biology of tauopathies. *Neuropathology* **2006**, *26*, 484−490.

(5) Braak, H.; Alafuzoff, I.; Arzberger, T.; Kretzschmar, H.; Del Tredici, K.; Staging of Alzheimer disease-associated neurofibrillary pathology using paraffin sections and immunocytochemistry. *Acta Neuropathol.* **2006**, *112*, 389−404.

(6) Jicha, G. A.; Parisi, J. E.; Dickson, D. W.; Johnson, K.; Cha, R.; Ivnik, R. J.; Tangalos, E. G.; Boeve, B. F.; Knopman, D. S.; Braak, H.; Petersen, R. C. Neuropathologic outcome of mild cognitive impairment following progression to clinical dementia. *Arch. Neurol.* **2006**, *63*, 674−81.

(7) Catalano, S. M.; Dodson, E. C.; Henze, D. A.; Joyce, J. G.; Krafft, G. A.; Kinney, G. G. The role of amyloid-beta derived diffusible ligands (ADDLs) in Alzheimer's disease. *Curr. Top. Med. Chem.* **2006**, *6*, 597−608.

(8) Hardy, J.; Selkoe, D. J. The amyloid hypothesis of Alzheimer's disease: Progress and problems on the road to therapeutics. *Science* **2002**, *297*, 353−356.

(9) Rosenberg, R. N. Explaining the cause of the amyloid burden in Alzheimer disease. *Arch. Neurol.* **2002**, *59*, 1367−1368.

(10) Thal, D. R.; Capetillo-Zarate, E.; Del, Tredici, K.; Braak, H. The development of amyloid beta protein deposits in the aged brain. *Sci. Aging Knowledge Environ.* **2006**, *2006*, re1.

(11) Blennow, K.; de Leon, M. J.; Zetterberg, H. Alzheimer's disease. *Lancet* **2006**, *368*, 387−403.

(12) Klunk, W. E.; Lopresti, B. J.; Ikonomovic, M. D.; Lefterov, I. M.; Koldamova, R. P.; Abrahamson, E. E.; Debnath, M. L.; Holt, D. P.; Huang, G. F.; Shao, L.; DeKosky, S. T.; Price, J. C.; Mathis, C. A. Binding of the positron emission tomography tracer Pittsburgh compound-B reflects the amount of amyloid-beta in Alzheimer's disease brain but not in transgenic mouse brain. *J. Neurosci.* **2005**, *25*, 10598−10606.

(13) Lopresti, B. J.; Klunk, W. E.; Mathis, C. A.; Hoge, J. A.; Ziolko, S. K.; Lu, X.; Meltzer, C. C.; Schimmel, K.; Tsopelas, N. D.; Dekosky, S. T.; Price, J. C. Simplified quantification of Pittsburgh compound B amyloid imaging PET studies: A comparative analysis. *J. Nucl. Med.* **2005**, *46*, 1959−1972.

(14) Mathis, C. A.; Klunk, W. E.; Price, J. C.; DeKosky, S. T. Imaging technology for neurodegenerative diseases: Progress toward detection of specific pathologies. *Arch. Neurol.* **2005**, *62*, 196−200.

(15) Price, J. C.; Klunk, W. E.; Lopresti, B. J.; Lu, X.; Hoge, J. A.; Ziolko, S. K.; Holt, D. P.; Meltzer, C. C.; DeKosky, S. T.; Mathis, C. A. Kinetic modeling of amyloid binding in humans using PET imaging and Pittsburgh compound B. *J. Cereb. Blood Flow Metab.* **2005**, *25*, 1528−1547.

(16) Ziolko, S. K.; Weissfeld, L. A.; Klunk, W. E.; Mathis, C. A.; Hoge, J. A.; Lopresti, B. J.; DeKosky, S. T.; Price, J. C. Evaluation of voxel-based methods for the statistical analysis of PIB PET amyloid imaging studies in Alzheimer's disease. *Neuroimage* **2006**, *33*, 94−102.

(17) Edison, P.; Archer, H. A.; Hinz, R.; Hammers, A.; Pavese, N.; Tai, Y. F.; Hotton, G.; Cutler, D.; Fox, N.; Kennedy, A.; Rossor, M.; Brooks, D. J. Amyloid, hypometabolism, and cognition in Alzheimer disease. An [11C]PIB and [18F]FDG PET study. *Neurology* **2007**, *68*, 501−508.

(18) Johnson, K. A. Amyloid imaging of Alzheimer's disease using Pittsburgh compound B. *Curr. Neurol. Neurosci. Rep.* **2006**, *6*, 496−503.

(19) Engler, H.; Forsberg, A.; Almkvist, O.; Blomquist, G.; Larsson, E.; Savitcheva, I.; Wall, A.; Ringheim, A.; Langstrom, B.; Nordberg, A. Two-year follow-up of amyloid deposition in patients with Alzheimer's disease. *Brain* **2006**, *129*, 2856−2866.

(20) Kemppainen, N. M.; Aalto, S.; Wilson, I. A.; Nagren, K.; Helin, S.; Bruck, A.; Oikonen, V.; Kailajarvi, M.; Scheinin, M.; Viitanen, M.; Parkkola, R.; Rinne, J. O. Voxel-based analysis of PET amyloid ligand [^{11}C]PIB uptake in Alzheimer disease. *Neurology* **2006**, *67*, 1575−1580.

(21) Mintun, M. A.; Larossa, G. N.; Sheline, Y. I.; Dence, C. S.; Lee, S. Y.; Mach, R. H.; Klunk, W. E.; Mathis, C. A.; DeKosky, S. T.; Morris, J. C. [11C]PIB in a nondemented population: Potential antecedent marker of Alzheimer disease. *Neurology* **2006**, *67*, 446−452.

(22) Nordberg, A. PET imaging of amyloid in Alzheimer's disease. *Lancet Neurol.* **2004**, *3*, 519−527.

(23) Buckner, R. L.; Snyder, A. Z.; Shannon, B. J.; LaRossa, G.; Sachs, R.; Fotenos, A. F.; Sheline, Y. I.; Klunk, W. E.; Mathis, C. A.; Morris, J. C.; Mintun, M. A. Molecular, structural, and functional characterization of Alzheimer's disease: evidence for a relationship between default activity, amyloid, and memory. *J. Neurosci.* **2005**, *25*, 7709−7717.

(24) Rentz, D. M.; Becker, J. A.; Moran, E.; Sperling, R. A.; Manning, L.; Bonab, A.; Mathis, C. A.; Klunk, W.; Fischman, A. J.; Johnson, K. A. Amyloid imaging in AD, MCI, and highly intelligent older adults with Pittsburgh compound B (PIB). *J. Nucl. Med.* **2006**, 289p (abstract).

(25) Price, J. C.; Ziolko, S. K.; Weissfeld, L. A.; William, K. E.; Bi, W.; Hoge, J. A.; Lopresti, B. J.; DeKosky, S. T.; Mathis, C. A. [O-15] Water and PIB PET imaging in Alzheimer's disease and mild cognitive impairment. *J. Nucl. Med.* **2006**, 75p (abstract).

(26) Villemagne, V. L.; Ng, S.; Gong, S. J.; Ackermann, U.; Pike, K.; Savage, G.; Klunk, W.; Mathis, C.; Masters, C. L.; Rowe, C. C. 11C-PIB PET imaging in the differential diagnosis of dementia. *J. Nucl. Med.* **2006**, 74p (abstract).

(27) Verhoeff, N. P.; Wilson, A. A.; Takeshita, S.; Trop, L.; Hussey, D.; Singh, K.; Kung, H. F.; Kung, M.-P.; Houle, S. In vivo imaging of Alzheimer disease beta-amyloid with [11C]SB-13 PET. *Am. J. Geriatr. Psychiatry* **2004**, *12*, 584−595.

(28) Small, G. W. Diagnostic issues in dementia: neuroimaging as a surrogate marker of disease. *J. Geriatr. Psychiatry Neurol.* **2006**, *19*, 180−185.

(29) Kepe, V.; Huang, S. C.; Small, G. W.; Satyamurthy, N.; Barrio, J. R. Visualizing pathology deposits in the living brain of patients with Alzheimer's disease. *Methods Enzymol.* **2006**, *412*, 144−160.

(30) Shoghi-Jadid, K.; Barrio, J. R.; Kepe, V.; Wu, H. M.; Small, G. W.; Phelps, M. E.; Huang, S. C. Imaging beta-amyloid fibrils in Alzheimer's disease: A critical analysis through simulation of amyloid fibril polymerization. *Nucl. Med. Biol.* **2005**, *32*, 337−351.

(31) Zhuang, Z.-P.; Kung, M.-P.; Hou, C.; Skovronsky, D.; Gur, T. L.; Trojanowski, J. Q.; Lee, V. M.-Y.; Kung, H. F. Radioiodinated styrylbenzenes and thioflavins as probes for amyloid aggregates. *J. Med. Chem.* **2001**, *44*, 1905−1914.

(32) Zhuang, Z.-P.; Kung, M.-P.; Hou, C.; Plossel, K.; Skovronsky, D.; Gur, T. L.; Trojanowski, J. Q.; Lee, V. M.-Y.; Kung, H. F. IBOX-(2-(4′-dimethylaminophenyl)-6-iodobenzoxazole): A ligand for imaging amyloid plaques in the brain. *Nucl. Med. Biol.* **2001**, *28*, 887−894.

(33) Wang, Y.; Klunk, W. E.; Debnath, M. L.; Huang, G. F.; Holt, D. P.; Shao, L.; Mathis, C. A. Development of a PET/SPECT agent for amyloid imaging in Alzheimer's disease. *J. Mol. Neurosci.* **2004**, *24*, 55−62.

(34) Kung, H. F.; Lee, C.-W.; Zhuang, Z. P.; Kung, M. P.; Hou, C.; Plossl, K. Novel stilbenes as probes for amyloid plaques. *J. Am. Chem. Soc.* **2001**, *123*, 12740−12741.

(35) Lee, C.-W.; Kung, M.-P.; Hou, C.; Kung, H. F. Dimethylamino-fluorenes: Ligands for detecting β-amyloid plaques in the brain. *Nucl. Med. Biol.* **2003**, *30*, 573−580.

(36) Zhuang, Z. P.; Kung, M. P.; Wilson, A.; Lee, C. W.; Plossl, K.; Hou, C.; Holtzman, D. M.; Kung, H. F. Structure−activity relationship of imidazo[1,2-a]pyridines as ligands for detecting beta-amyloid plaques in the brain. *J. Med. Chem.* **2003**, *46*, 237−243.

(37) Kung, M.-P.; Hou, C.; Zhuang, Z.-P.; Skovronsky, D.; Kung, H. F. Binding of two potential imaging agents targeting amyloid plaques in postmortem brain tissues of patients with Alzheimer's disease. *Brain Res.* **2004**, *1025*, 89−105.

(38) Kung, M.-P.; Hou, C.; Zhuang, Z.-P.; Cross, A. J.; Maier, D. L.; Kung, H. F. Characterization of IMPY as a potential imaging agent for β-amyloid plaques in double transgenic PSAPP mice. *Eur. J. Nucl. Med. Mol. Imaging* **2004**, *31*, 1136−1145.

(39) Newberg, A. B.; Wintering, N. A.; Plossl, K.; Hochold, J.; Stabin, M. G.; Watson, M.; Skovronsky, D.; Clark, C. M.; Kung, M. P.; Kung, H. F. Safety, biodistribution, and dosimetry of 123I-IMPY: A novel amyloid plaque-imaging agent for the diagnosis of Alzheimer's disease. *J. Nucl. Med.* **2006**, *47*, 748−754.

(40) Newberg, A. B.; Wintering, N. A.; Clark, C. M.; Plossl, K.; Skovronsky, D.; Seibyl, J. P.; Kung, M. P.; Kung, H. F. Use of 123I IMPY SPECT to differentiate Alzheimer's disease from controls. *J. Nucl. Med.* **2006**, *47*, p. 78 (Abstract # 220).

(41) Zhang, W.; Oya, S.; Kung, M. P.; Hou, C.; Maier, D. L.; Kung, H. F. F-18 Stilbenes as PET imaging agents for detecting beta-amyloid plaques in the brain. *J. Med. Chem.* **2005**, *48*, 5980−5988.

(42) Zhang, W.; Oya, S.; Kung, M. P.; Hou, C.; Maier, D. L.; Kung, H. F. F-18 PEG stilbenes as PET imaging agents targeting Aβ aggregates in the brain. *Nucl. Med. Biol.* **2005**, *32*, 799−809.

(43) Zhang, W.; Kung, M. P.; Oya, S.; Hou, C.; Kung, H. F. F-18 labeled styrylpyridines as PET agents for amyloid plaque imaging. *Nucl. Med. Biol.* **2007**, in press.

(44) Ono, M.; Haratake, M.; Nakayama, M.; Kaneko, Y.; Kawabata, K.; Mori, H.; Kung, M. P.; Kung, H. F. Synthesis and biological evaluation of (E)-3-styrylpyridine derivatives as amyloid imaging agents for Alzheimer's disease. *Nucl. Med. Biol.* **2005**, *32*, 329−35.

(45) Meana, A.; Rodriguez, J. F.; Sanz-Tejedor, M. A.; Garcia-Ruano, J. L. Efficient regioselective preparation of monobromo- and bromoiodo-hydroxypyridines from dibromo derivatives via bromine−lithium exchange. *Synlett* **2003**, 1678−1682.

(46) Comins, D. L.; Jianhua, G. N-vs. O-alkylation in the Mitsunobu reaction of 2-pyridone. *Tetrahedron Lett.* **1994**, *35*, 2819−2822.

(47) Cunico, R. F.; Bedell, L. The triisopropylsilyl group as a hydroxyl-protecting function. *J. Org. Chem.* **1980**, *45*, 4797−4798.

(48) Jeffery, T.; Ferber, B. One-pot palladium-catalyzed highly chemo-, regio-, and stereoselective synthesis of trans-stilbene derivatives. A concise and convenient synthesis of resveratrol. *Tetrahedron Lett.* **2002**, *44*, 193−197.

(49) Jeffery, T. On the efficiency of tetraalkylammonium salts in Heck type reactions. *Tetrahedron* **1996**, *52*, 10113−10130.

(50) Hervet, M.; Thery, I.; Gueiffier, A.; Enguehard-gueiffier, C. Comparative study on the reactivity of 6-haloimidazo[1,2-a]pyridine derivatives towards Negishi- and Stille-coupling reactions. *Helv. Chim. Acta* **2003**, *86*, 3461−3469.

(51) Wnuk, S. F.; Yuan, C.-S.; Borchardt, R. T.; Balzarini, J.; De Clercq, E.; Robins, M. J. Nucleic acid-related compounds. 84. Synthesis of 6′-(E and Z)-halohomovinyl derivatives of adenosine, inactivation of S-adenosyl-L-homocysteine hydrolase, and correlation of anticancer and antiviral potencies with enzyme inhibition. *J. Med. Chem.* **1994**, *37*, 3579−3587.

(52) Bastiaans, H. M. M.; van der Baan, J. L.; Ottenheijm, H. C. J. Flexible and convergent total synthesis of cyclotheonamide B. *J. Org. Chem.* **1997**, *62*, 3880−3889.

(53) Ono, M.; Wilson, A.; Nobrega, J.; Westaway, D.; Verhoeff, P.; Zhuang, Z. P.; Kung, M. P.; Kung, H. F. ^{11}C-Labeled stilbene derivatives as Aβ-aggregate-specific PET imaging agents for Alzheimer's disease. *Nucl. Med. Biol.* **2003**, *30*, 565−571.

(54) Mathis, C. A.; Wang, Y.; Holt, D. P.; Huang, G.-f.; Debnath, M. L.; Klunk, W. E. Synthesis and evaluation of ^{11}C-labeled 6-substituted 2-arylbenzothiazoles as amyloid imaging agents. *J. Med. Chem.* **2003**, *46*, 2740−2754.

(55) Mathis, C. A.; Wang, Y.; Klunk, W. E. Imaging β-amyloid plaques and neurofibrillary tangles in the aging human brain. *Curr. Pharm. Des.* **2004**, *10*, 1469−1492.

(56) Kung, M. P.; Hou, C.; Oya, S.; Mu, M.; Acton, P. D.; Kung, H. F. Characterization of [123I]IDAM as a novel single-photon emission tomography tracer for serotonin transporters. *Eur. J. Nucl. Med.* **1999**, *26*, 844−853.